J. Physiol. (Paris) 94 (2000) 357–374

PII: S0928-4257(00)01101-3/REV

Reliable circuits from irregular neurons: A dynamical approach to understanding central pattern generators

Allen I. Selverston*, Mikhail I. Rabinovich, Henry D.I. Abarbanel, Robert Elson, Attila Szücs, Reynaldo D. Pinto, Ramón Huerta, Pablo Varona

Institute for Nonlinear Science, University of California, San Diego, 9500 Gilman Drive, La Jolla, CA 92093-0402, USA

Abstract – Central pattern generating neurons from the lobster stomatogastric ganglion were analyzed using new nonlinear methods. The LP neuron was found to have only four or five degrees of freedom in the isolated condition and displayed chaotic behavior. We show that this chaotic behavior could be regularized by periodic pulses of negative current injected into the neuron or by coupling it to another neuron via inhibitory connections. We used both a modified Hindmarsh-Rose model to simulate the neurons behavior phenomenologically and a more realistic conductance-based model so that the modeling could be linked to the experimental observations. Both models were able to capture the dynamics of the neuron behavior better than previous models. We used the Hindmarsh-Rose model as the basis for building electronic neurons which could then be integrated into the biological circuitry. Such neurons were able to rescue patterns which had been disabled by removing key biological neurons from the circuit. © 2000 Elsevier Science Ltd. Published by Éditions scientifiques et médicales Elsevier SAS

central pattern generator / neural modeling / nonlinear systems electronic neurons / chaotic behavior

1. Introduction

Central pattern generating circuits (CPGs) are neural networks specialized for the production of rhythmic motor patterns. Found in all nervous systems, they have evolved to produce rhythmic spatio-temporal motor patterns independently, i.e. without the need of rhythmic sensory feedback [4]. Of course the patterns are strongly influenced by sensory feedback as well as by chemical neuromodulatory substances, but the fundamental structure of the pattern is determined by the synaptic connections and biophysical properties of the individual neurons. These properties are crucial in determining the timing and organization of the motor patterns. They can be altered chemically so that, by exposing CPGs to chemical modulators always present in nervous systems, they can be functionally reconfigured, so that one anatomical circuit can produce many different stable modes of activity. This presents an analytical challenge since in intact animals the properties of CNS neurons are in a constant state of flux [9]. In general, CPGs require the presence of one or more modulators to function in a normal manner and if completely free of modulatory influence will usually be inoperative. So the challenge is to provide CPGs with enough modulation to be rhythmically active and then hold the chemical environment constant so that the rhythms will be stable for extended periods. Depending on the particular chemical modulators present, a large number of different patterns can be generated. During these stable regimes, however they must still be flexible enough to respond to sensory input from the environment. Most circuits of model neurons are unable to simulate this important property.

Invertebrate CPGs have been shown to be very useful for studying the mechanisms of pattern generation because they are particularly amenable to experimental analysis and they are usually made up of limited numbers of relatively large neurons that can be repeatedly identified from one animal to another. The part of the nervous system containing the CPG machinery can be removed from the rest of the animal, thus reducing or entirely eliminating the changes caused by the chemical substances they are exposed to normally. Using small CPG systems, paired recordings can be made from the same identified neurons in different preparations and their synaptic connectivity established. Recording from pre- and postsynaptic neurons has uncovered the circuitry for many small CPGs. We suggest that the neural patterns these CPGs generate are robust and reliable in the face of noise and external perturbations even though, as we will demonstrate, individual neurons in the circuit may behave chaotically. By behaving chaot-

* Correspondence and reprints.

E-mail address: aselverston@ucsd.edu (A.I. Selverston).

ically we mean that when isolated from all synaptic input from other neurons and subjected to both linear and nonlinear analysis, they not only demonstrate irregularities in their membrane potential bursting/spiking firing patterns, but also demonstrate deterministic chaos in their phase space attractors, Lyanopov exponents and entropy measurements.

To investigate this thesis, we have begun to analyze the pattern generating mechanisms of the lobster pyloric rhythm using new analytical techniques. We have been working on two CPGs, the gastric and the pyloric, from the lobster stomatogastric system, for over 30 years [9, 18, 19]. The gastric CPG is the more complex of the two and operates the three teeth of the gastric mill. The pyloric CPG is the faster rhythm and operates a filtering mechanism at the lower end of the stomach. Although driving movements of the stomach, the muscles involved are striated and require continuous control from the CNS. While the physiological details of both circuits are known, it cannot be said that we understand, by any rigorous formulation, how the motor patterns are produced, i.e. at a reductionistic level we know the physiological properties of the cells and synapses, but the total operation of the network is an 'emergent property' that is more than the sum of its parts. This is especially the case for CPGs where most of the properties are nonlinear and dynamic.

We have analyzed the pyloric CPG because we believe that by understanding the patterns produced by this small system, we will gain some insights as to how larger circuits in the brain are able to generate spatio-temporal patterns. Our approach relies heavily on being able to move seamlessly between experiment and theory. At the present time it is not possible to prove or disprove the validity of large scale modeling of the brain since untestable assumptions are made with regards to synaptic connectivity and cellular properties, general phenomena which are essential in making useful and informative models. We seek to provide a rigorous formulation of the underlying principles by modeling a well-defined system. Our models mimic the output of a biological CPG not just in the steady state, but during a variety of perturbations as well. We are particularly interested in capturing the dynamical properties of the biological systems. The models are simple enough to study with available mathematical and computational techniques. We have been applying these new modeling and nonlinear analysis methods to the lobster pyloric CPG in order to try and answer several fundamental questions:

– How can a CPG, made up of neurons which produce chaotic voltage oscillations, generate regular spatio-temporal rhythmic activity patterns that are stable, robust and reliable in the presence of noise, yet flexible enough to provide specific and reproducible responses to inputs?
– If there is chaos in CPG systems, what role does it play during normal behavior?
– How many degrees of freedom are needed for modeling a biological CPG accurately? i.e. how many equations will capture the biological behavior?
– We know that in intact systems neurons fire more regularly than when isolated. What are the mechanisms that achieve this regularization in intact GPG systems?

Our strategy has been to first determine the dynamical properties of single neurons in the pyloric circuit after they have been synaptically isolated from the other neurons. Thus, if the isolated neurons show chaotic behavior, we can be sure it is not the result of nonlinear synaptic interactions. We then examine how these isolated neurons can become regularized by various kinds of synaptic inputs from other neurons or by periodic pulses of current. We then extend the analysis by constructing mathematical models of the pyloric neurons that reproduce the dynamical aspects of isolated cells and small subsets of cells both in steady state and perturbed conditions. Finally we describe an in silico model of neurons, i.e. electronic neurons that though elegantly simple, appear to capture all of the essential dynamical features of membrane potential in their biological counterparts. We examine the properties of their individual behaviors under a variety of perturbations as well as examining their behaviors in pairs and in hybrid circuits with biological neurons.

2. Dynamical properties of biological neurons

Neurons in the pyloric CPG circuit are synaptically connected as shown in *figure 1*. There are fourteen neurons in the circuit, all motor neurons except AB, which is an interneuron. When the circuit receives neuromodulatory input from two upstream ganglia, the commissurals (CGs), the membrane potentials of all of the neurons show bursting-spiking activity, i.e. they are what are termed conditional oscillators, conditional upon the presence of modulators that activate the underlying bursting currents. The oscillatory activity is somewhat irregular in each individual neuron, but

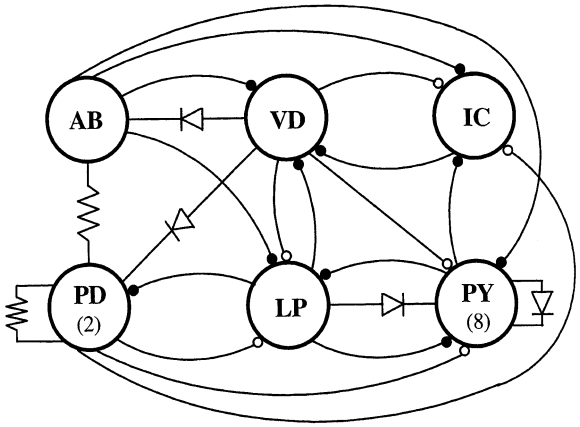

Figure 1. Electronic equivalent circuit for the lobster pyloric central pattern generator. Black dots represent chemical synapses and resistors represent electrotonic connections. There are two pyloric dilator neurons (PD), one lateral pyloric (LP), one ventricular dilator (VD), one inferior cardiac (IC) and eight pyloric neurons (PY). All of the neurons except the anterior burster (AB), are motor neurons as well as pattern forming neurons.

becomes more regularized when the neurons are embedded in a network and receive synaptic input (mostly inhibitory) from other neurons in the circuit. The AB interneuron is the only neuron which, when isolated, has periodic regular bursting activity. Because the AB's activity has the highest natural frequency, it also serves as the pacemaker for the entire pyloric network. The neurons comprising the pyloric network are typical of both vertebrate motorneurons and spinal interneurons in that they contain large numbers of channels, receptors and synaptic mechanisms [9].

We selected the LP neuron for detailed analysis because it appeared to be typical of many pyloric motor neurons and a large amount of information about this particular neuron already existed [8]. Intracellular time series lasting several hours were sampled at a data rate of 2 kHz (*figure 2:1*). The Fourier power spectrum for this time series was broadband without separate peaks as is typical in cases of a chaotic time series, and did not reveal anything about the dynamics underlying the intracellular voltage signal. A nonlinear analysis however suggested that by using the method of false nearest neighbors [1], the active degrees of freedom for the LP neuron are only four or five. This suggests we can make models of the behavior of this neuron with only five degrees of freedom. This was a remarkable finding because neurons contain

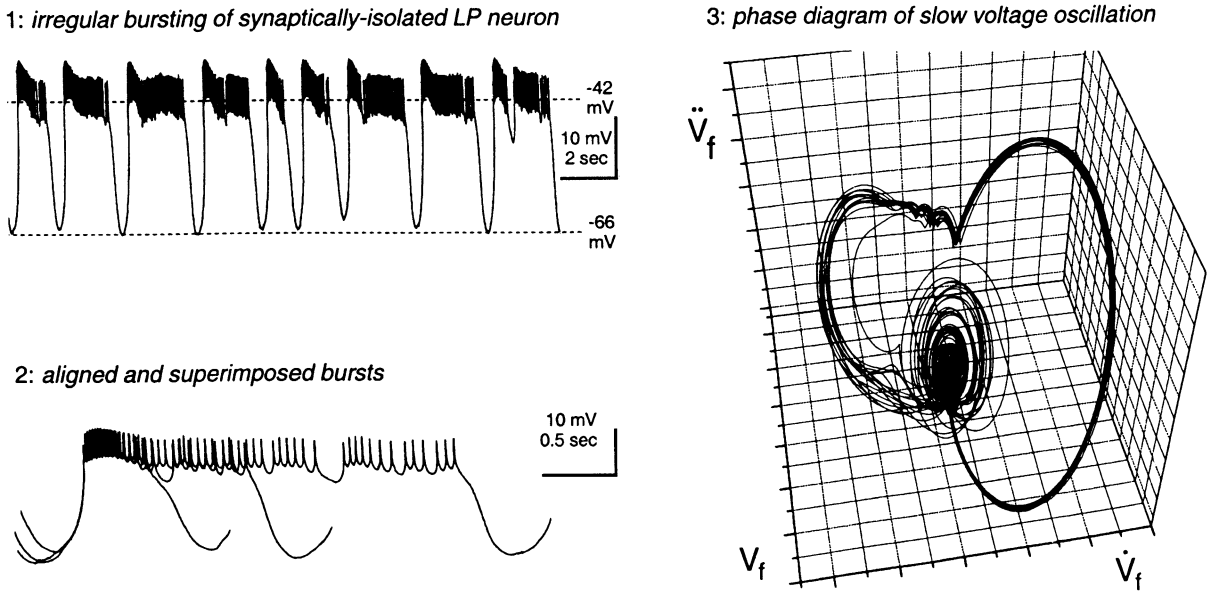

Figure 2. Irregular spontaneous bursting in a synaptically isolated LP neuron still receiving modulatory input from the commissural ganglia. (1) Excerpt from an extended time series showing a typical irregular bursting pattern. (2) Three bursts aligned by their first spike and superimposed. (3) Phase space diagram of slow voltage oscillations from a time- series of a similarly isolated LP. The membrane potential [$V(t)$] was low-pass filtered to remove the spikes. The plot of $V(t)$ against its first and second derivatives reconstructs an attractor showing, in addition to noise, apparent deterministic structure. The motion in time is counter-clockwise. The large orbit corresponds to the overall slow wave (from burst to burst), the smaller spiral to faster oscillations on the plateau (during each burst).

many more than five fast and slow dynamical processes and therefore usually considerably more than four or five equations are thought to be necessary for an adequate model. Modifications of the original Hodgkin-Huxley equations [12] to include the dynamics of more recently discovered channels are a good example. This finding opened up two possible options for us to pursue. On the one hand we could use rather simple phenomenological models that might capture the dynamics of the neuron but would be inappropriate for modeling experimental data. On the other hand we could utilize models which incorporate mathematical descriptions of the principle ionic channels necessary for more realistic simulations. We have tried both approaches.

When the analysis of the LP time series data was complete, it showed that the isolated neuron had a positive global Lyapunov exponent, a hallmark of chaotic behavior in a dynamical system. In another study in which we made slight perturbations to the orbit, we found that there were two positive global Lyapunov exponents, one zero exponent suggesting the behavior is governed by ordinary differential equations, and two negative exponents. A fractal dimension of approximately 4.4 was established based on these global exponents. Chaotic neurons in invertebrates have been reported previously [10, 13] but their analysis was much less detailed. Chaotic oscillations are a possible state of activity when many ion channels having different kinetic properties are operating, but in fact many typical Hodgkin-Huxley type models show little chaos.

One may speculate as to the actual usefulness of chaos in small systems — the ability to explore wider domains of high dimensional space than if constrained to a limit cycle for example, but the fact is that when neurons are embedded in a complex synaptic circuit, they behave in a much more regular way than when they are isolated. The networks made up of these unstable neurons operate in a reliable and predictible fashion but are robust enough to resist strong perturbations. CPGs that produce rhythmic motor patterns for cyclic behaviors must contain a reliable system for providing impulses to the appropriate muscles. It is clearly important then to determine the mechanisms involved in achieving this degree of regularity and stability from what are inherently unstable elements without losing the ability of the CPGs to respond to sensory and command elements or their ability to restructure themselves into functionally new networks under the influence of neuromodulators. Therefore we decided to initially examine the regularizing effects of various forms of current injection, both natural and artificial, into isolated pyloric neurons which were displaying chaotic activity.

2.1. Regularization of chaotic neurons

We have studied the LP neuron by characterizing its dynamic response to periodic current pulses, sinusoidal driving and phasic inhibitory input from presynaptic pacemaker neurons. Experimental perturbations were applied to isolated neurons and the resulting time series were analyzed using an entropy measure obtained from the power spectra. As previously noted, when the LP was isolated from phasic inhibitory input, it generated irregular spiking-bursting activity. Each burst begins in a relatively stereotyped manner, but then evolves with exponentially increasing variability (*figure 2:2*) [6] This can also be seen in the chaotic attractor (*figure 2:3*).

2.2. Regularizion of chaotic activity by current pulses

We found that depolarizing current pulses were poor regulators of the neurons but the hyperpolarizing pulses were able to exert a strong, frequency-dependent regularizing action. The LP was synaptically isolated from other neurons in the pyloric circuit by photoinactivating the PD and VD neurons (because they are cholinergic and cannot be specifically blocked pharmacologically) and blocking the remaining glutamatergic synapses with picrotoxin. The CGs were left connected to the stomatogastric ganglion via the stomatogastric nerve so the isolated LP would receive the same neuromodulators it receives under normal experimental conditions. Long time series traces (5–6 min) of membrane voltage were digitized and the degree of irregularity in the observed oscillations was determined from the power spectra and a measure of the entropy for the harmonics of the power spectra for frequencies up to 40 Hz.

Fast Fourier spectra were calculated from the digitized voltage signals without filtering and the power in harmonics up to 40 Hz, $P(n)$ for $n =$ 20 976 were converted to probability values as $p(n) = P(n)/\Sigma P(n)$.

An entropy function (in bits), $S = -\Sigma_n p(n)\log_2[p(n)]$, was then evaluated. S gives a quantitative measure of the complexity of the power spectrum associated with the observed time

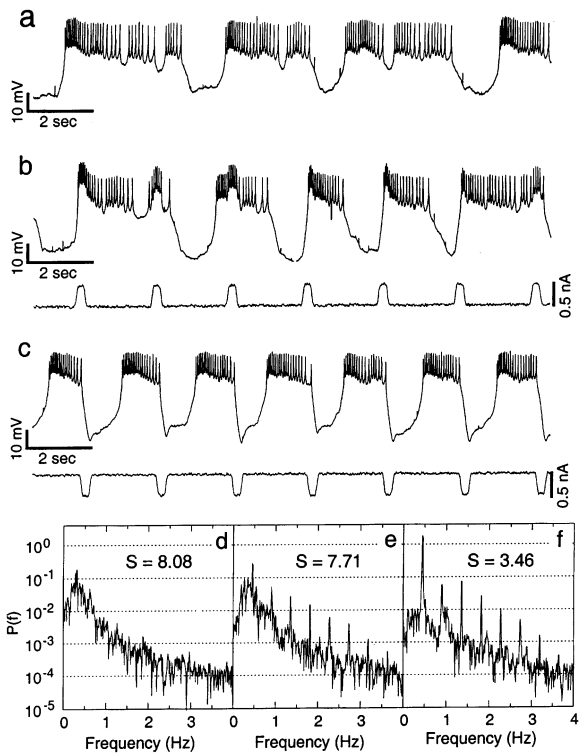

Figure 3. Regularization of irregular bursting activity by injection of periodic current pulses. Recordings (**a–c**) and analysis (**d–f**) of voltage activity in an LP neuron after removal of chemical synaptic input from other pyloric neurons. (**a**) Free running control activity. (**b**) Forcing by periodic depolarizing current pulses (frequency, 0.45 Hz). (**c**) Forcing by periodic hyperpolarizing current pulses at the same frequency. (**d**) Fourier power spectrum for control activity. (**e**) Spectrum for depolarizing pulses. (**f**) Spectrum for hyperpolarizing pulses. Entropy values (S) are given in bits. Conditions: VD and both PDs killed; PTX; 1 mM 4-AP.

series. By this measure, a power spectrum with a single peak (a linear periodic system) yields $S = 0$ bits. A spectrum with two isolated peaks (a linear quasi-periodic system with two possible states) $S = 1$ bit, a flat or white noise spectrum extending to 40 Hz (or $n = 20\,976$) yields $S = \log_2(20\,976) = 14.35$ bits. Low values of S, relative to 14.35 bits, are then interpreted as associated with lower complexity in the oscillations of the system.

As shown in *figure 3a*, *d*, an isolated but still modulated LP neuron behaves irregularly with an entropy S value of 8.08 bits and a power spectrum which shows a wide distribution and a broad peak. When current pulses were applied at a slightly higher frequency than the free-running neuron, 0.45 Hz, to approximate excitatory input, there were changes to the timing and duration of the bursts as might be expected, but little change in the irregularity (*figure 3b*). The entropy dropped only to 7.71 and there was little change to the power spectrum aside from the addition of local peaks at the stimulus frequency and it's multiples (*figure 3e*). Hyperpolarizing current pulses meant to mimic inhibitory input had a much more powerful effect on regularizing the bursts (*figure 3c*). As shown in *figure 3c*, *f*, entropy was reduced to 3.46 bits and the power spectrum was concentrated into sharp peaks at the applied frequency and its harmonics.

The mechanism underlying the stabilization appears to be due to the hyperpolarizing current terminating the plateau potentials before instabilities in the burst phase occur. The initial stable phase of the burst can also be extended until the arrival of the next inhibitory input.

2.3. Regularization of LP by biological pacemaker inhibition

We also examined the way in which the LP neuron could be regularized by biological inhibitory input. To do this we experimentally produced a subcircuit consisting of the pacemaker group consisting of the electrotonically-coupled AB and PD neurons, and the LP neuron. The VD neuron was photoinactivated and removed from the network and all other synapses once again blocked with picrotoxin. This left the PDs with their inhibitory inputs to the LP intact and by direct current injection we could alter the frequency of bursting in the AB-PD pacemaker group. If we examine the effects of the PD forcing at different frequencies (*figure 4*), it is clear that the spontaneous pacemaker input regularized the free-running chaotic activity of LP in a frequency-dependent manner.

During spontaneous activity of the subcircuit, the LP displayed a power spectrum with strong peaks at the PD spontaneous frequency and its harmonics. The LP entropy was reduced to $S = 5.1$ bits [6]. The LP was also able to follow at lower frequencies but as the forcing frequency was reduced, the LP power spectra broadened and lost structure. When the PDs were shut of entirely, the LP activity displayed a broadband structure and the entropy increased to $S = 7.9$ bits, essentially the same as above.

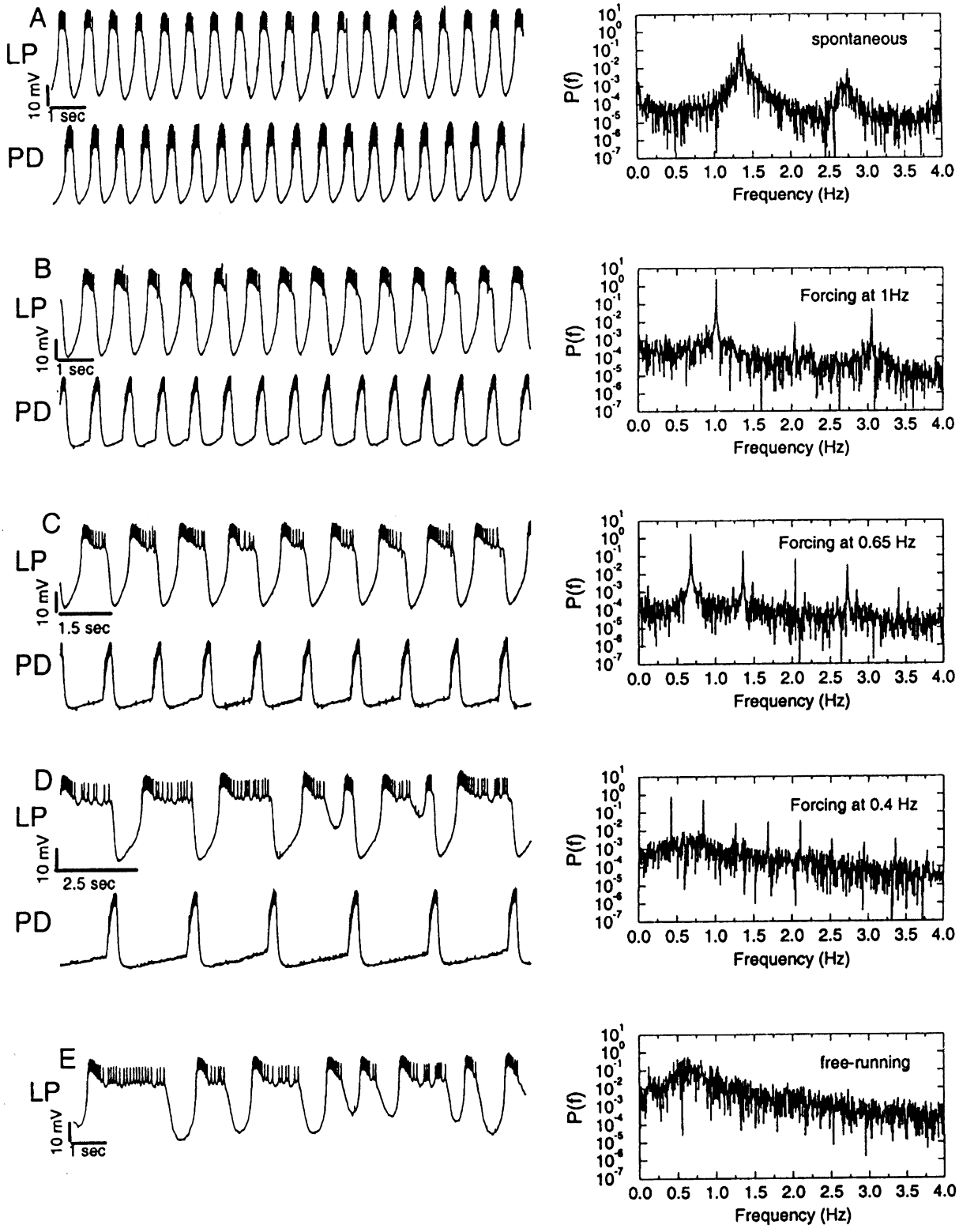
A
LP
10 mV
1 sec
PD
spontaneous
P(f)
Frequency (Hz)
B
LP
10 mV
1 sec
PD
Forcing at 1Hz
P(f)
Frequency (Hz)
C
LP
10 mV
1.5 sec
PD
Forcing at 0.65 Hz
P(f)
Frequency (Hz)
D
LP
10 mV
2.5 sec
PD
Forcing at 0.4 Hz
P(f)
Frequency (Hz)
E
LP
10 mV
1 sec
free-running
P(f)
Frequency (Hz)

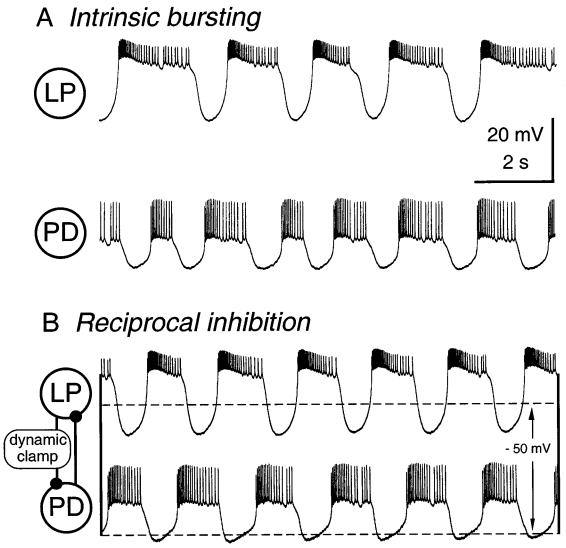

Figure 5. Reciprocal synaptic inhibition regularizes the chaotic bursting of LP and a single PD neuron. (**A**) Intrinsic bursting of LP and PD neurons recorded (at different times in the same experiment) while isolated from circuit interactions. (**B**) The same two neurons coupled by reciprocal inhibition. The LP-to-PD connection is inserted via a dynamic clamp. Conditions: AB, VD and one PD photoinactivated; PTX. In (**A**), the LP recording was made with the remaining PD deeply hyperpolarized.

2.4. Mutual regularization by reciprocal inhibition

Can chaotically bursting neurons regularize each other? When the AB neuron is killed, the PDs also burst irregularly (*figure 5A*). When PD and LP inhibited each other via their normal connectivity, they adopted anti-phase coordination and regularized their bursting (*figure 5B*). What with all natural synapses blocked, and with simulated synapses inserted via the dynamic clamp [21], we could show that only reciprocal inhibition (not any other pattern of connectivity) could produce regularization (unpublished data).

2.5. Synchronization and regularization by electrotonic coupling

Electrotonic coupling exists between many neurons in the STG. We studied the dynamical effects of adding artificial electrical coupling in parallel to the natural coupling between the two PD neurons,

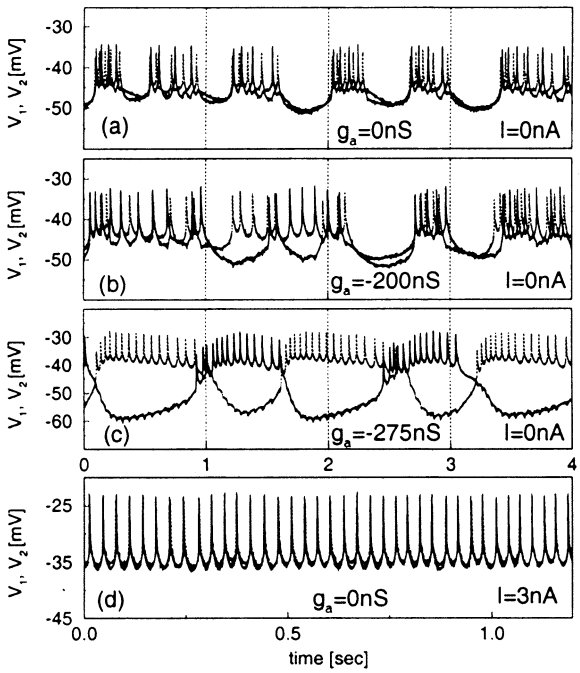

Figure 6. Regimes of oscillations in two coupled neurons. (**a**) With no applied current, the slow oscillations are synchronized while the spikes are not (**b**) counteracting the natural coupling leads to independent bursting (**c**) with net negative coupling, the neurons burst in anti-phase in a regular pattern (**d**) when depolarized by a positive depolarizing current, both neurons fire a continuous pattern of synchronized spikes. In the figure, g_a is the added synaptic conductance and I the current injected into the two neurons.

again using a dynamic current clamp device. The effective coupling could be altered by injecting equal and opposite current (I_a) into each cell via microelectrodes such that $I_a^{(j)} = g_a(V_j - V_i)$, where g_a is the added synaptic conductance and V_I is the membrane potential at the soma PD_I [20]. Typical records for added conductances are shown in (*figure 6*) [5]. The natural coupling of these neurons synchronized bursts but not individual spikes (*figure 6a*). The natural coupling was sufficient to synchronize spikes during the tonic firing (*figure 6d*) implying a shunting action of slow membrane conductances during burst generation. Opposing the natural coupling via the dynamic clamp causes the bursting to become more asynchronous (*figure*

Figure 4. Control of irregular bursting by rhythmic synaptic inhibition: intracellular recordings and Fourier power spectra. In this configuration, the only strong phasic synaptic input to LP comes from the PD neurons which are part of the pacemaker group. The rhythmic bursting of the pacemakers was altered by current injection. Left column: simultaneous intracellular recordings from LP and PD neurons. Right column: corresponding Fourier power $[P(f)]$ spectra for the LP membrane potential, evaluated from long time series. The displayed frequency range encompasses the slower voltage oscillations. (**A**) Spontaneous activity of subcircuit. (**B**) PD forced to burst at 1 Hz. (**C**) PD forcing at 0.65 Hz. (**D**) PD forcing at 0.4 Hz. (**E**) Free running activity of LP when PD bursting was shut off by strong hyperpolarization.

6b) finally leading to out-of-phase bursting and increased regularization (*figure 6c*). In this case the net negative coupling approximates reciprocal inhibition.

3. Computational and electronic modeling of STG neurons

Because our analysis of biological neurons had shown they could be modeled with only three or four degrees of freedom, we chose initially to use a familiar simplified model put forward by Hindmarsh and Rose (HR) [11]. The general form of this model contains three terms:

$$dx/dt = ay(t) + bx^2(t) - cx^3(t) - dz(t) + I \quad (1)$$

$$dy/dt = e - fx^2(t) - f(t) \quad (2)$$

$$dz/dt = \mu[-z(t) + S(x(t) + h)] \quad (3)$$

The first three equations represent the original model where $x(t)$ corresponds to membrane voltage, $y(t)$ represents a 'fast' current and by making $\mu \ll 1$, $z(t)$ a 'slow' current. The first three equations (the 3-D model) can produce several modes of spiking-bursting activity including a regime of chaos that appears similar to that seen in biological neurons.

However the parameter space for the chaotic behavior is much more restricted than we observe in real neurons. The chaotic regime is greatly expanded by incorporation of the fourth term into the model:

$$dw/dt = v[-kw(t) + r(y(t) + 1)] \quad (4)$$

Adding this term $w(t)$ to introduce an even slower process ($v < \mu \ll 1$) is intended to represent intracellular Ca dynamics. Note this also adds a $-gw(t)$ to the second equation. When this term is taken into account, the model produces simulations of intracellular activity that are even more similar to the biological observations. We, as yet, do not know if the $w(t)$ term actually represents Ca kinetics in pyloric neurons and experiments are currently under way to measure Ca transients in neurons using optical methods.

Because of its relative simplicity, the HR model was extremely useful in constructing an analog implementation — an electronic neuron — that could perform the computations necessary to emulate stomatogastric neurons in real time. However the down side of such a simplified model is that it is difficult to compare with biological neurons which are made up of a multitude of individual conductances and compartments. Since the experimental manipulation of these parameters is crucial in establishing physiological mechanisms, we also developed a Hodgkin-Huxley (H-H) type model that is more biologically realistic than that of Hindmarsh and Rose. In this second model [7], the neuron is represented by two compartments, one for the lumped neuropilar processes and soma and the other for the axon. The currents we have used are based on previous descriptions [3, 23] but are restricted to those that we consider to be the most important in generating slow wave and spiking current. In all, five currents are present in the soma-neuropil compartment (I_{Ca1} low voltage activated calcium current, I_{Ca2} high voltage activated calcium current, I_h hyperpolarization-activated inward current, $I_{K(Ca)}$ calcium dependent potassium current, and a leak current I_L). The axonal compartment contains the well-known Hodgkin-Huxley currents for spiking – I_{Na}, I_K, and a leak current I_L. The soma-neuropil compartment also incorporates intracellular dynamics based on the model of Li et al. [13]. In this model, cytosolic (Ca^{2+}) is determined by influx across the plasma membrane and by uptake and release from the ER and extrusion by a plasma membrane pump and a plasma membrane Na-Ca exchanger.

3.1. Modeling of single neurons

The three-dimensional H-R model generates a time series that looks remarkably similar to the time series of an isolated LP neuron (*figures 2–4*, *7*), and its strange attractor has the same topology as the one shown in *figure 2*. Even without an equation for the slow Ca dynamics, the model contains the appropriate mix of slow and fast dynamics to accurately describe the bursting spiking behavior seen in single isolated pyloric neurons.

The soma voltage time series trajectories shown by the Hodgkin-Huxley-calcium model were also quite similar to those observed in biological neurons [8]. In both cases, the most common feature was the variability in burst duration. In isolated LP neurons, the burst periods were in the range of 1–3 s and for the model in the range of 1.5–3 s with the most frequent period being about 1.7 s. In the H-H calcium dynamics model, the soma compartment produces plateau depolarizations that produce spiking in the axon compartment. Ca plays a key role in determining the length of the plateau and therefore the length of the burst. The plateau potential is maintained in the model by the competition between the inward currents [7].

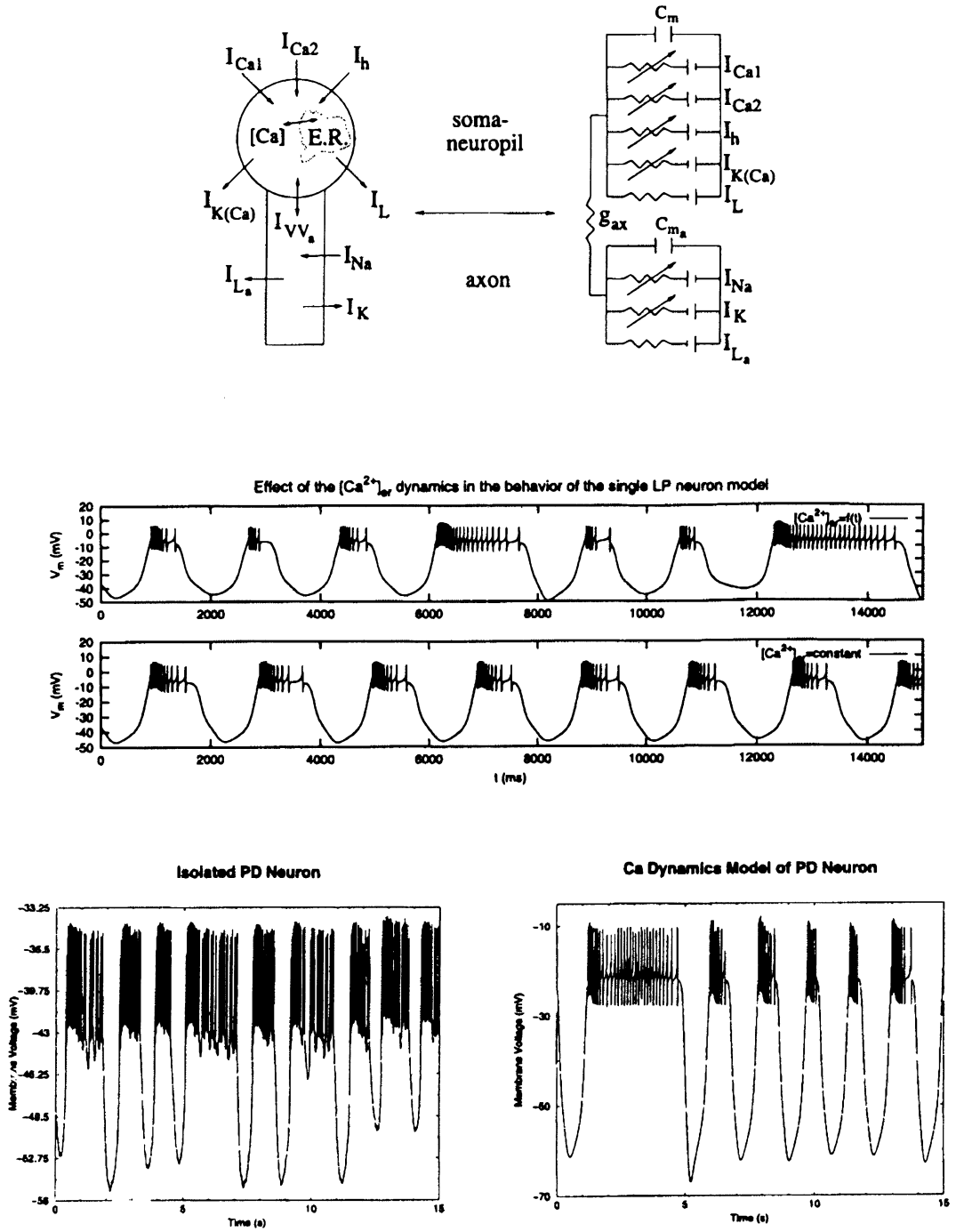

Figure 7. A Hodgkin-Huxley plus calcium conductance-type model made up of two compartments simulates the irregular bursting of the LP neuron. The location of the conductances is shown on the cell diagram and their electronic circuit counterpart is shown on the right. Changes in burst dynamics can be produced by raising the cytoplasmic calcium concentration (middle panel). The lower panel shows a comparison between the burst activity produced by the model (right) and a biological neuron (left).

3.2. Synchronization in two inhibitory coupled model H-R neurons

The simplest minimal circuit that we studied consisted of two identical synaptically coupled neurons. We started by looking at inhibitory synapses because they represent the predominant synaptic type in the stomatogastric system and because there has been considerable theoretical work on reciprocal inhibition as the basis for alternate bursting in rhythmic motor systems. In addition, inhibitory synapses appear to play a major role in coordinating the timing of bursts in rhythmic systems and in regulating the dynamics of coupled chaotic neurons. We characterized coupled H-R neurons as having a threshold and a constant resting potential and added to the equation describing the membrane potential x_1 of one neuron a synaptic current associated with the action of another neuron with potential x_2 to give:

$$I_s = -[\varepsilon + \eta(t)][x_1(t) + V_c]\theta[x_2(t - \tau_c) - X]$$

where ε is the strength of the coupling and $\eta(t)$ a small zero mean noise term. The model shows several different regions of synchronization depending on the values of synaptic strength and synaptic delay. When both are small, there is a region of complete in-phase synchronization. As the strength is increased, the neurons become less synchronized until they fire out-of-phase with one another. The inhibitory coupling reliably regularized the behavior of the individually chaotic neurons except when the coupling was very weak.

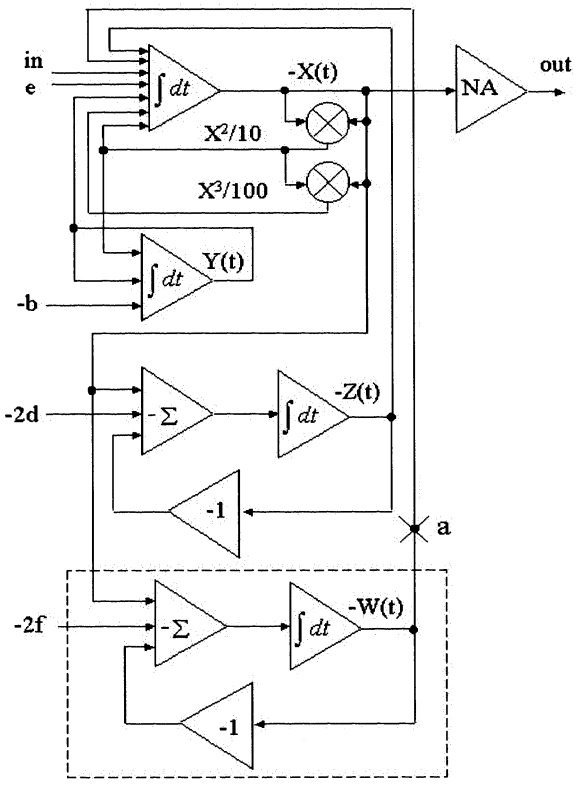

Figure 8. Block diagram of the four-dimensional HR + Ca^{2+} neuron used in our experiments. These neurons were based on the equations shown in the text and were designed to replicate the behavior of individual isolated neurons from the lobster STG. In our experiments the electronic neurons were coupled to each other electrically as well as via an electronic implementation of inhibitory and excitatory chemical synapses.

4. Electronic neurons

Using three and four-dimensional Hindmarsh-Rose models, we have constructed low dimensional analog electronic neurons (ENs) whose properties emulate the membrane voltage characteristics of individual stomatogastric neurons [16]. The ENs are simple analog circuits which integrate the four-dimensional differential equations representing fast and slow subcellular mechanisms that produce the characteristic regular/chaotic spiking-bursting behavior of these cells. A schematic diagram for the EN is shown in *figure 8*. Our strategy for building an analog device instead of using numerical integration of the mathematical model on a PC or DSP board was due to the fact that digital integration of the H-H equations is a slow procedure associated with the two or three different time scales in the model We also plan to eventually construct real-time networks of the entire pyloric CPG and for a large number of neurons and for this, analog implementation is a necessity.

4.1. Behavior of the single electronic neuron

As mentioned previously, the equation for $w(t)$ represents an even slower process than $z(t)$ so that $\nu < \mu \ll 1$ and is included because a slow process such as the calcium exchange between intracellular stores and the cytoplasm was found to be required in Hodgkin-Huxley modeling [7] to fully reproduce the observed chaotic oscillations of STG neurons. Both the three-dimensional and four-dimensional models have regions of chaotic behavior, but the four-dimensional model has much larger regions in parameter space where chaos occurs presumably for the many of the same reasons that calcium dynamics give rise to chaos in HH modeling

(*figure 7*). The main parameters we used in controlling the modes of spiking and bursting activity of the model are the DC external current I and the time constants μ and v of the slow variables (*figure 9*). The Lyapunov exponents λ_I for both the 3-D and 4-D ENs have positive exponents in both cases indicating conclusively that the behavior of the model was chaotic.

4.2. Synaptic connections between ENS

In order to study the functional relationships between ENs, we also developed circuits to simulate excitatory and inhibitory synaptic connections as well as ohmic electrical connections. Electrical synapses were implemented by injecting a current into one of the neurons proportional to the voltage

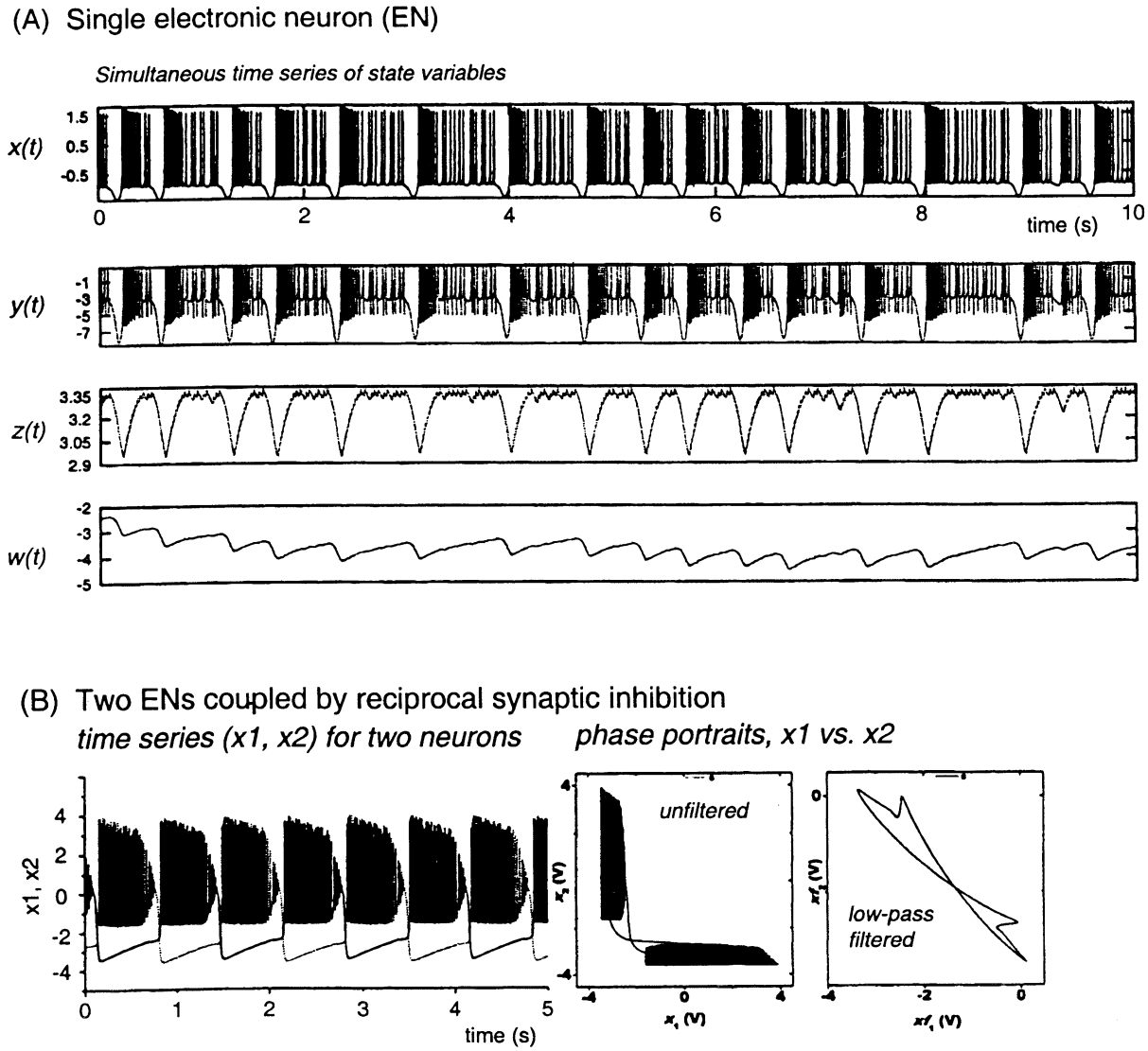

Figure 9. The electrical behavior of an electronic neuron. **A** shows a simultaneous time series of the computed state variables x (membrane potential), y (fast conductance), z (slow conductance) and w (cytosolic calcium concentration). **B** shows the simulated activated of two ENs coupled by synaptic inhibition and their phase portraits.

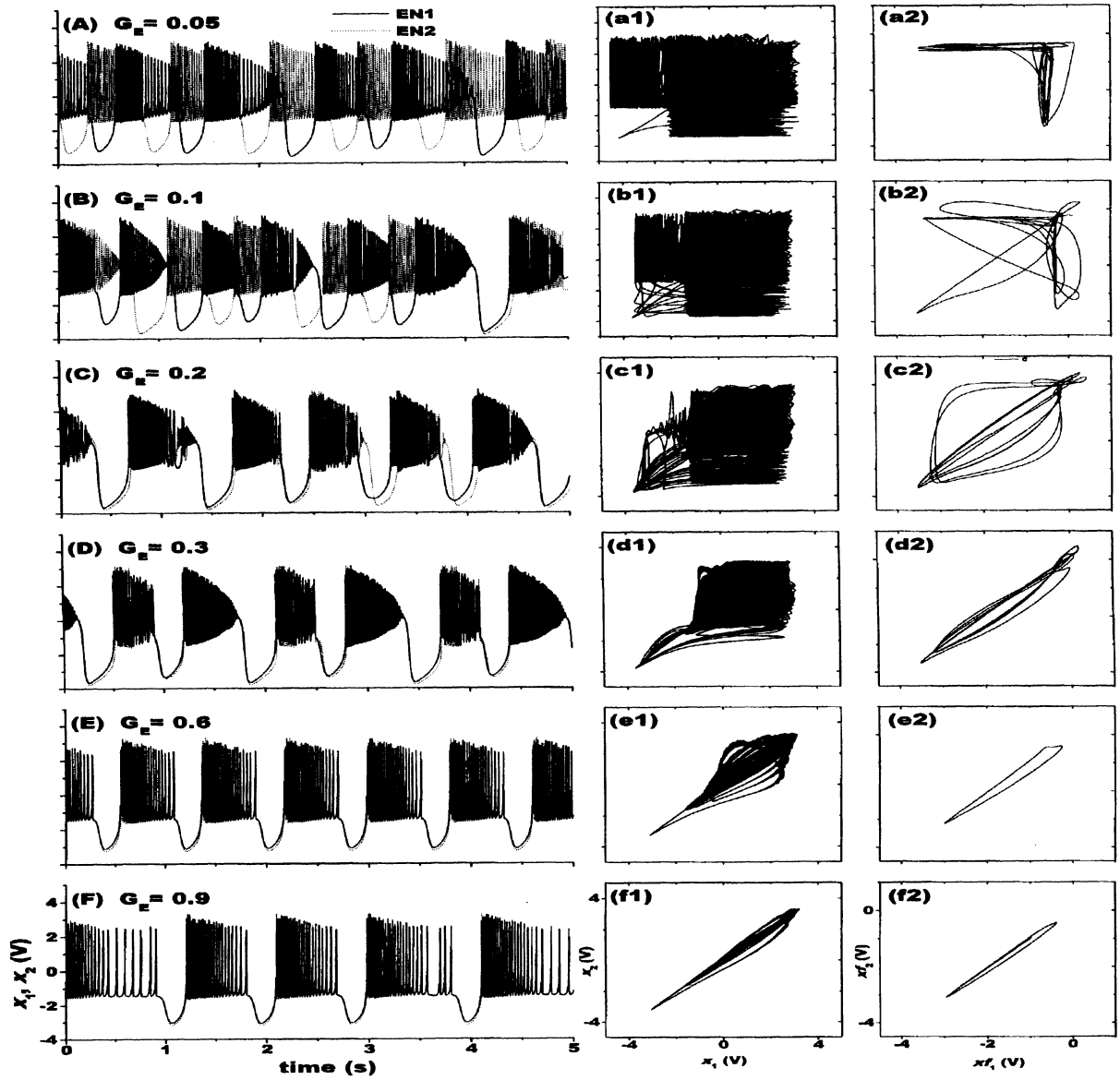

Figure 10. Positive electrical coupling of two chaotic ENs. Characteristic time series of the membrane potentials $x_1(t)$, $x_2(t)$ [**A**–**F**] as synaptic conductance G_E is varied. Phase portraits (a1–f1) are shown on the right unfiltered and after low pass filtering (a2–f2). (**A**) Intermittent out-of-phase activity, (**B**) nearly independent chaotic spiking-bursting pattern, (**C**) chaotic oscillations with most bursts synchronized, (**D**) periodic oscillations with partial synchronization of the ENs, spikes not synchronized, (**E**) periodic oscillations with complete synchronization of the ENs, (**F**) chaotic but completely synchronized oscillations.

difference between the two membrane potentials and injecting the same current with the opposite polarity into the other neuron.

Although chemical synapses could be implemented in analog circuitry, we found it more useful to use software so that we could investigate the

Figure 11. Inhibitory chemical coupling between two chaotic ENs. Characteristic time series of the membrane potentials (**A**–**F**). Phase portraits (a1 to e1) and phase portraits after 20 Hz low-pass filtering (a2 to e2). (**A**) Chaotic oscillations with all hyperpolarized regions out-of-phase, (**B**) periodic pattern with hyperpolarizing regions out-of-phase and some burst superposition, (**C**) chaotic oscillations, (**D**) periodic out-of-phase bursting behavior with some burst superposition, (**E**) periodic out-of-phase spiking-bursting behavior, (**F**) chaotic out-of-phase spiking-bursting pattern.

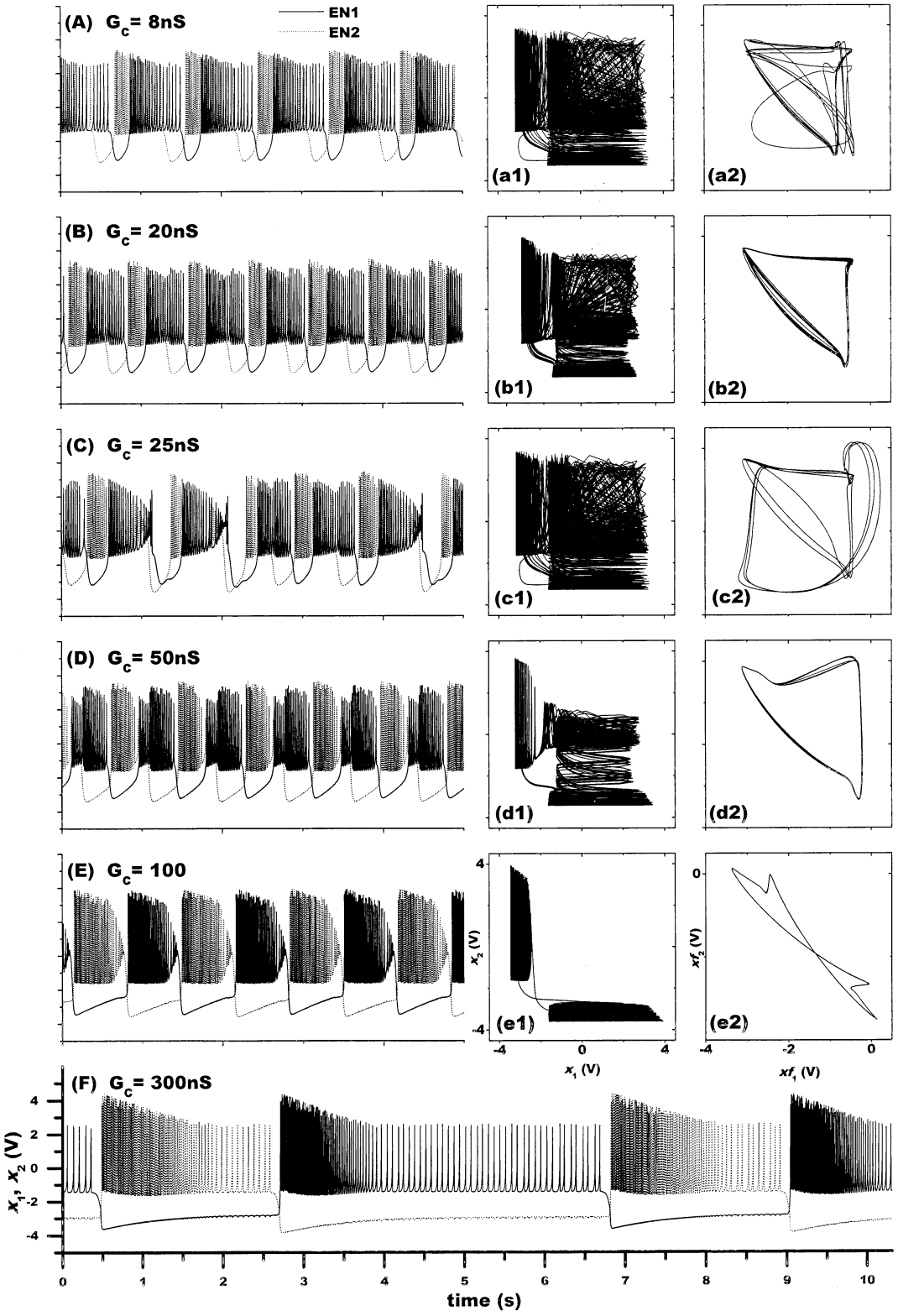
(A) G_c= 8nS
EN1
EN2
(a1)
(a2)
(B) G_c= 20nS
(b1)
(b2)
(C) G_c= 25nS
(c1)
(c2)
(D) G_c= 50nS
(d1)
(d2)
(E) G_c= 100
(e1)
(e2)
x_2 (V)
x_1 (V)
xf_2 (V)
xf_1 (V)
(F) G_c= 300nS
x_1, x_2 (V)
time (s)

role of the synaptic time constant τ_s. We found the results of the software and hardware models were identical for fixed time constants. The electronic neurons were able to generate the currents corresponding to the graded chemical synapses of STG neurons in real time described by first order kinetics. The synaptic reversal potentials were selected so that the currents injected into the postsynaptic ENs were always negative for inhibitory synapses and positive for excitatory synapses.

4.3. Electrical coupling between two ENs

When the coupling strength $G_E \approx 0.0$, the two neurons are effectively uncoupled and display independent chaotic oscillations. However as the strength of the coupling increases, some regions of synchronized bursting begins to appear (*figure 10*) including regions where intermittent anti-phase bursting can be observed. As the coupling is made stronger the bursting activity becomes regular and goes from a region of partial synchronization to a region of total synchronization. Between values of 0.8 and 1, there is total synchronization in the spiking bursting activity and the oscillations are chaotic. For negative electrotonic coupling, something that does not occur in nature, the oscillations are mostly chaotic and the bursts occur in anti-phase. As with experiments on biological neurons, there is a sharp phase transition between nearly synchronous and fully synchronous behavior [15].

4.4. Excitatory chemical-type synapses between ENs

When two uncoupled ENs were adjusted to give independent chaotic oscillations, they became regularized as they transitioned between simulated currents $0 < G_C < 100$ nS. At very low currents (10 nS) the chaotic activity was replaced by a behavior in which most of the bursts were synchronized but the oscillations were still chaotic. At 100 nS all the bursts became synchronized and the activity becomes periodic. At $G_C > 100$ nS the bursts remain synchronized and get longer but there are no longer any spikes during the final part of the bursts.

4.5. Inhibitory chemical-type synapses between ENs

ENs connected with reciprocal chemical inhibitory synapses mimic the most common form of communication between pattern forming neurons in CPGs. We suggested previously that inhibitory chemical coupling could lead to regularization of chaotic oscillations in individual neurons [2]. We found that with small inhibitory currents the EN oscillations were still chaotic and all of the hyperpolarizing regions of the membrane voltages were in anti-phase (*figure 11*). As the strength of the inhibitory synapses were increased, the oscillations became alternately periodic and chaotic until at very high synaptic currents long out-of-phase bursts were observed along with chaotic oscillations. While these results are consistent with what we have observed in biological neurons, no direct comparison of these simulations with biological neurons has been made. When very strong inhibi-

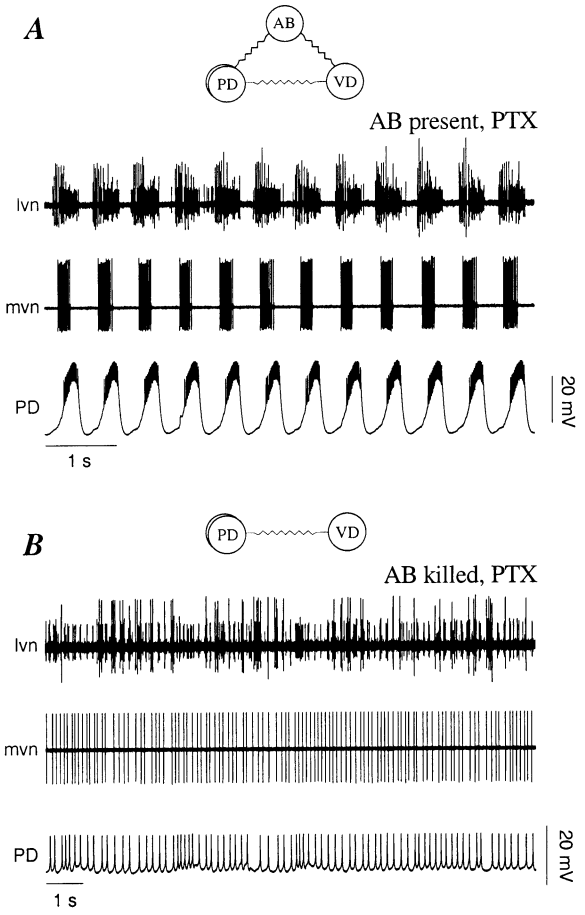

Figure 12. The pyloric pacemaker group, the AB and PDs along with the VD neuron are able to sustain bursting after the glutamatergic synapses are blocked with picrotoxin (**A**) however when the AB is photoinactivated (**B**) the remaining neurons become tonic initially and after about one hour resume bursting activity.

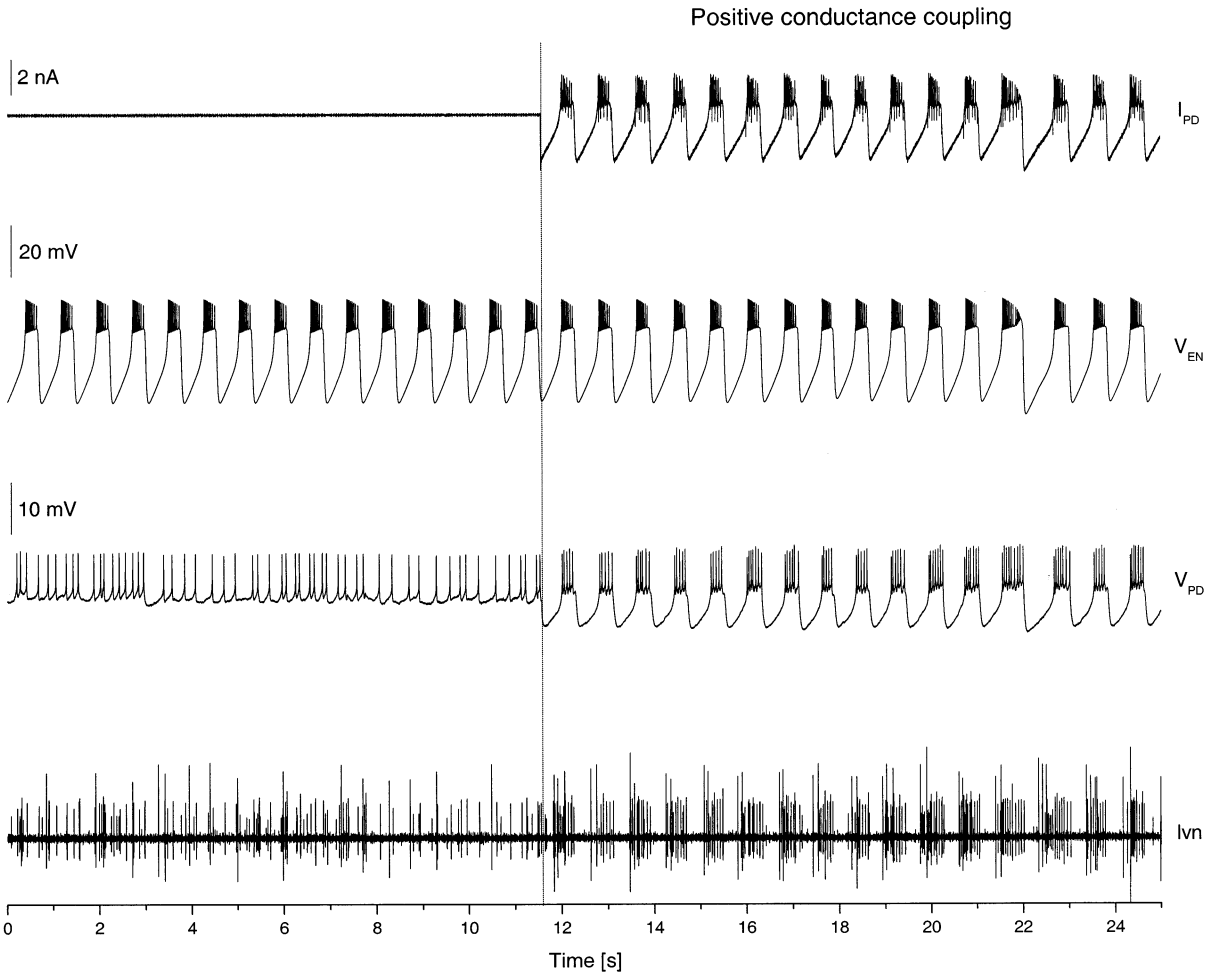

Figure 13. A hybrid circuit in which a EN that is firing like AB is inserted into a biological circuit in which AB has been killed. Prior to the vertical line in the center, the current between the EN and the PDs is shut off and the pyloric rhythm is tonic as shown in the PD intracellular trace and extracellular LVN trace. After the positive conductance coupling is turned on as shown in the top trace, the pyloric pattern is reinstituted.

tion is delivered via a dynamic clamp, I_h is activated sufficiently to keep the oscillations regular (unpublished).

4.6. Hybrid silicon-biological circuits

One way to test the verisimilitude of our ENs was to interface them with single biological neurons or with the entire pyloric circuit. It would then be possible in principle to see if the EN could substitute for the real neuron under a variety of perturbations as well as in steady state conditions. The pyloric system is exceptionally well-suited for these experiments. The fourteen neuron pyloric network has one interneuron, the AB, that is connected to the two PD neurons via electrotonic junctions (see *figure 1*). Together these three neurons appear to form the pacemaker for the pyloric system, setting the frequency and periodicity of the pyloric pattern. The AB is the strongest neuron of the three in this respect and because it is robust and highly periodic it has been difficult to manipulate the rhythm when it is intact.

The AB can be removed from the pyloric circuit by photoinactivation [14] and in some cases glutamatergic transmission from other pyloric neurons onto the PDs was blocked with picrotoxin (7.5 μM). A three-dimensional EN was connected to the two PD neurons via an artificial electrical synapse [22] which allowed us to dynamically in-

teract with the biological neurons rather than simply providing them with current commands through a microelectrode.

When the AB was removed from a reduced circuit leaving only the PDs still connected to the VD neuron, the normal oscillatory pattern was immediately disrupted and the PD and VD fired tonically and irregularly (*figure 12*). If the EN was adjusted to fire in bursts similar to those observed in the AB and then connected to the PDs by an artificial electrical synapse, the PD now fired synchronously with the EN (*figure 13*). When the EN is also made to fire irregularly and then connected to the chaotically firing PDs, the ENs and the PDs went immediately into synchronous in-phase bursting/firing activity (*figure 14A*).

Similarly, if the electrical coupling was made negative, bursting/firing activity also ensued but now was out-of-phase (*figure 14B*). If the glutamatergic activity was blocked, the whole rhythm became severely disrupted immediately after the AB pacemaker neuron was photoinactivated. After about 1 h, the pyloric rhythm again become regularized although not as strongly as before. Replacing the destroyed AB with an artificial AB could rescue the circuit and the entire rhythm returned (*figure 15*). Experiments were also carried out using a 4-D EN with similar results [16].

Previous efforts using hybrid circuits have been performed using a digital version of a H-H model which ran on a DSP board of a PC and was used to replace PD, LP and PY neurons. This hybrid circuit demonstrated that many aspects of the pyloric rhythm could be accurately reproduced [17]. This laboratory subsequently developed VLSI devices for implementing HH type models and has used them in hybrid circuits with results similar to ours but we have found that thus far such complex neurons are not needed in order to retain the output properties and dynamical features of the network.

Modeling with hybrid circuits is an interesting way of testing how well an electronic neuron can interact with a small numbers of neurons in a well-characterized biological CPG. So far, our silicon neuron having only four degrees of freedom appears to be capable of behaving indistinguishably from its biological counterparts. We therefore

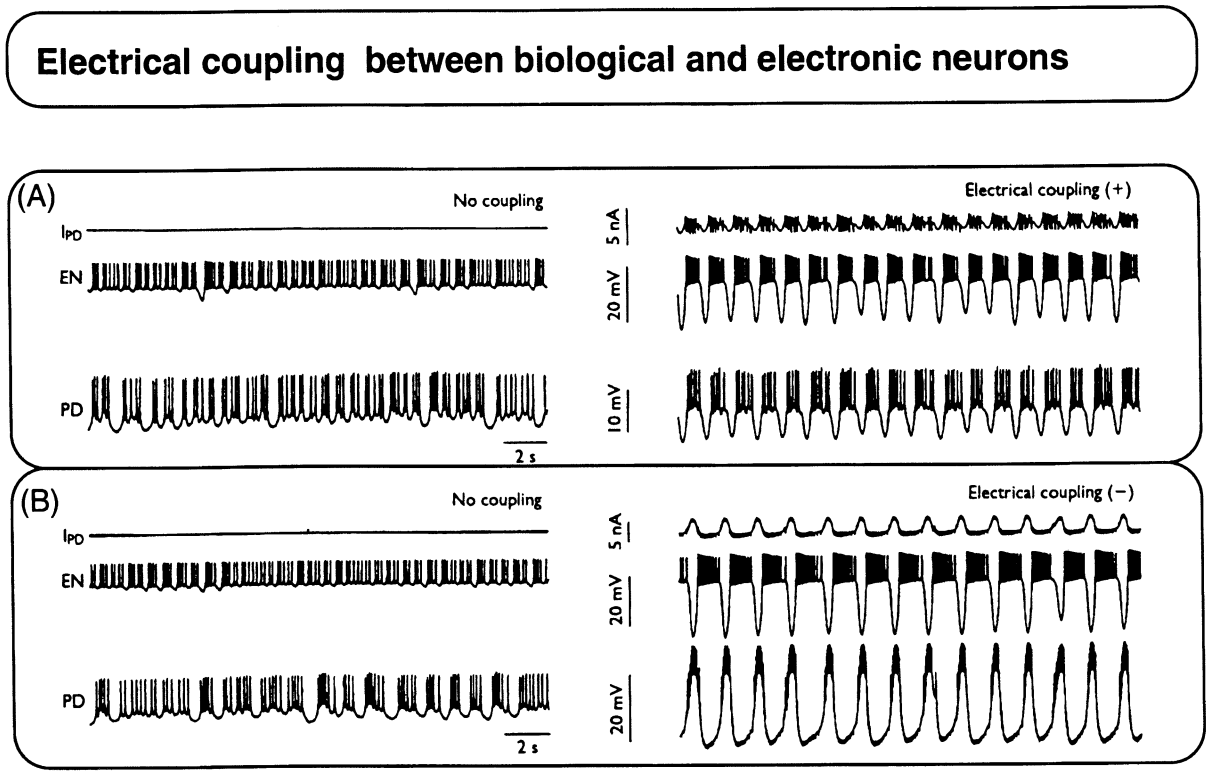

Figure 14. Hybrid circuit in which an irregular EN is coupled to an irregular biological PD neuron via positive (**A**) and negative (**B**) conductance coupling. The coupling produces an in-phase and out-of-phase periodic bursting/spiking pattern in the two neurons.

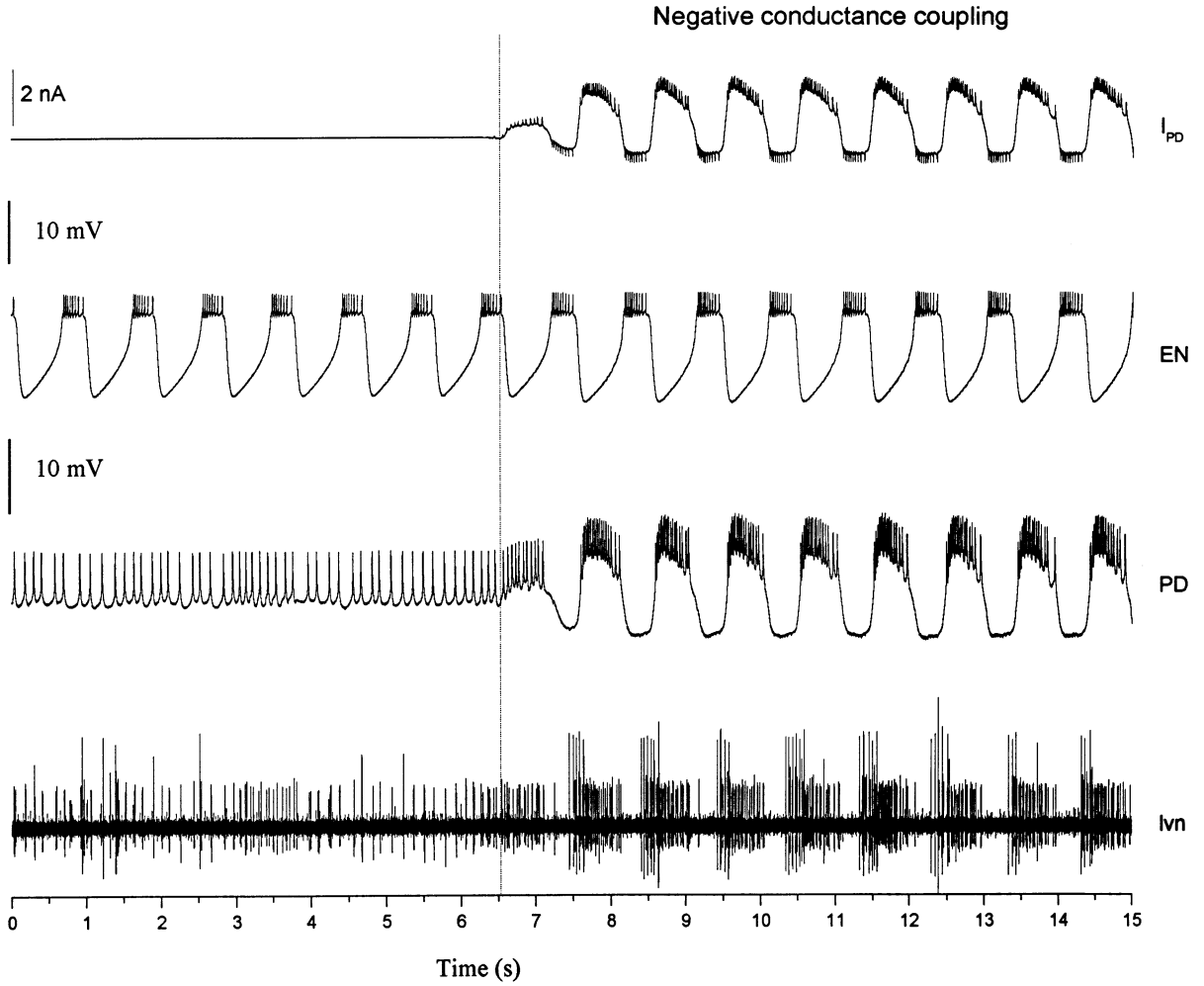

Figure 15. Same as *figure 13* but with negative conductance coupling which can also restart the pyloric rhythm. Note the EN and PD are out-of-phase in this non-biological condition.

appear to have captured enough of the salient features of real neurons to allow their substitution into a small biological network or we have not yet tested the electronic neuron hard enough to expose its frailties. We find it remarkable however that our ENs are not only able to drive the biological neurons but are also influenced by them as well i.e., they actually become part of the CPG circuitry.

5. Conclusions

– The individual neurons in an invertebrate CPG circuit have membrane potential behaviors that vary from periodic to irregular but for non-transient behaviors, they act as low dimensional oscillators.

– Irregularly firing neurons coupled to each other via inhibitory synapses tend to regularize better than neurons with excitatory coupling.

– The modified Hindmarsh-Rose model appears to be able to capture the essential dynamical features of stomatogastric neurons and can serve as the basis for constructing analog electronic neurons which operate in real time.

– Such simple electronic neurons, when interfaced with biological circuits, behave at the level of membrane potentials, like neurons.

– The Hodgkin-Huxley model with added Ca dynamics (1) displays biologically realistic chaotic regimes and (2) can be used to explore the underlying cellular mechanisms which produce chaos

and (3) is better than the H-R model in terms of linking experimental data with theoretical results.

We now know that chaotic neurons are much more reliable and diverse in their properties than was once believed. We have shown in our experiments that a very small collection of chaotic neurons can form an adaptive and flexible pattern generator which is very sensitive to sensory and central sources of input.

How does nature use chaos and how do small neural networks like invertebrate CPGs with chaotic neurons produce such beautifully regular patterns? We believe we have begun to answer that question with the experiments presented here. Of course a chaotic neuron may not actually have a function as such and may be chaotic simply because it is itself a complex nonlinear system. And questions remains — do CPGs use chaos to their advantage or do they try to minimize it? Do stochastic processes influence the dynamic behavior of nerve cells? Nonlinear dynamics gives neurons the flexibility and information processing abilities that allow them to perform new kinds of activities. The limit cycle attractors of highly periodic oscillators are rigid while unstable trajectories use more degrees of freedom — needed if flexibility and reliability are to be achieved. It appears that nature has opted for the more flexible approach.

References

[1] Abarbanel H.D.I., Analysis of observed chaotic data, Springer Verlag, New York, 1996.

[2] Abarbanel H.D.I., et al., Synchronized action of synaptically coupled chaotic neurons: I. Simulations using model neurons, Nerual. Comput. 8 (1996) 1567–1602.

[3] Buchholtz F., et al., Mathematical model of an identified stomatogastric ganglion neuron, 67 (1992) 332–340.

[4] Delcomyn F., Natural basis of rhythmic behavior in animals, Science 210 (1980) 492–498.

[5] Elson R.C., et al., Synchoronous behavior of two coupled biological neurons, Phys. Rev. Lett. 81 (1998) 5692–5695.

[6] Elson R.C., et al., Dynamic control of irregular bursting in an identified neuron of an oscillatory circuit, J. Neurophysiol. 82 (1999) 115–122.

[7] Falke M., et al., Modeling observed chaotic oscillations in bursting neurons: the role of calcium dynamics and IP3, Biol. Cyber. 82 v) 517–527.

[8] Golowasch J., Marder E., Ionic currents of the lateral pyloric neuron of the stomatogastric ganglion of the crab, J. Neurophysiol. 67 (1992) 318–331.

[9] Harris-Warrick R.M., et al. (Eds.), Dynamic Biological Networks: The Stomatogastric Nervous System, MIT Press, Cambridge, 1992.

[10] Hayashi H., Ishizuka S., Chaotic nature of bursting discharges in the Onchidium pacemaker neuron, J. Theor. Biol. 156 (1992) 269–291.

[11] Hindmarsh J.L., Rose R.M., A model of neuronal bursting using three coupled first order differential equations, Proc. R. Soc. Lond. B 221 (1984) 87–102.

[12] Hodgkin A., Huxley A., A quantitative description of membrane current and its application to conduction and excitation in nerve, J. Physiol. 117 (1952) 500–544.

[13] Li Y.-X., et al., Sensing and refilling calcium stores in an excitable cell, Biophys. J. 72 (1997) 1080–1091.

[14] Miller J.P., Selverston A.I., Rapid killing of single neurons by irradiation of intracellularly injected dye, 206 (1979) 702–704.

[15] Mpitsos G.J., et al., Evidence for chaos in spike trains of neurons that generate rhythmic motor patterns, Brain Res. Bull. 21 (1988) 529–538.

[16] Pinto R.D., et al., Phys. Rev. E (2000) (in press).

[17] Renaud-LeMasson S., et al., Hybrid circuits of interacting computer model and biological neurons, in: Hanson S.J., Cowan J.D., Giles C.L. (Eds.), Advances in Neural Information Processing systems 5, Morgan Kaufman, San Mateo, CA, 1993, pp. 813–819.

[18] Selverston A.I., et al., The stomatogastric nervous system: structure and function of a small neural network, Prog. Neurobiol. 7 (1976) 215–290.

[19] Selverston A.I., Moulins M. (Eds.), The Crustacean Stomatogastric System, Springer-Verlag, Berlin, 1987.

[20] Sharp A., Abbott L.F., Marder E., Artificial electrical synapses in oscillatory neurons, J. Neurophysiol. 67 (1992) 1691–1694.

[21] Sharp A.A., et al., Dynamic clamp: computer-generated conductances in real neurons, J. Neurophysiol. 69 (1993) 992–995.

[22] Szucs A., et al., Interacting biological and electronic neurons generate realistic oscillatory rhythms, Neuroreport 11 (2000) 563–569.

[23] Turrigiano G., LeMasson G., Marder E., Selective regulation of current densities underlines spontaneous changes in the activity of cultured neurons, J. Neurosci. 15 (1995) 3640–3652.